J Mater Sci (2007) 42:3055–3065
DOI 10.1007/s10853-006-0584-8

Durability of alkali-activated fly ash cementitious materials

A. Fernandez-Jimenez · I. García-Lodeiro · A. Palomo

Received: 9 January 2006 / Accepted: 16 June 2006 / / Published online: 14 December 2006

Abstract The study described in the present paper addresses the durability of alkali-activated fly ash (AAFA) cement under different conditions: specifically, cement performance is measured in a number of aggressive environments (deionized water, ASTM seawater, sodium sulphate and acidic solutions) and with respect to alkali–silica reaction-induced expansion. The chief parameters studied are: weight loss, compressive strength, variations in volume, presence of the products of degradation and microstructural changes. The results show that AAFA pastes perform satisfactorily in aggressive environments and that degradation in these materials is distinctly different from such processes in OPC paste. These mortars are also compliant with the 16-day expansion limit stipulated in ASTM standard C1260-94 on potential alkali–silica reactivity.

Introduction

The alkali activation of fly ash is a chemical process in which this industrial by-product, mixed with highly alkaline solutions and subjected to mild thermal curing (50–100 °C), sets and hardens, giving rise to a material with good cementitious properties [1–3]. The steadily increasing flow of papers published on the use of these materials in the construction industry stands as evidence of the enormous interest they have sparked in the scientific community.

Today there is a wealth of literature on the key factors affecting the alkali activation of fly ash (AAFA) [4–6] and the mechanisms controlling that process [7–9]. And many authors agree that these materials are remarkably resistant to acid attack [10–12].

Palomo et al. [11] reported that mortars made with alkali-activated metakaolin perform very stably when immersed in aggressive solutions of various types (deionized water, ASTM seawater, sodium sulphate solution and sulphuric acid). The transformation of the amorphous aluminosilicate network into a crystalline structure can be partly attributed to duration of the treatment (immersion). While representing a relatively small proportion of these crystals, faujasites—which would appear to reinforce the cement matrix—account for the steady increases in its mechanical strength after 90 days of immersion.

Bakharev et al. [12, 13], and Van Jaarsveld et al. [14, 15] in turn, sustained that the stability of AAFA pastes in aggressive environments depended on the intrinsic ordering of the components within the aluminosilicate gel. They found that geopolymer materials prepared with sodium hydroxide are more crystalline than when prepared with sodium silicate activators And the greater the crystallinity the more stable were the geopolymers in aggressive environments, such as sulphuric and acetic acid solutions. He attributed these findings to the formation of a more stable cross-linked aluminosilicate polymer structure when the activator used was sodium hydroxide. In any event, AAFA mortar was observed to perform better than ordinary

A. Fernandez-Jimenez · I. García-Lodeiro · A. Palomo (✉)
Eduardo Torroja Institute (CSIC), 4 Serrano Galvache St., 28080 Madrid, Spain
e-mail: palomo@ietcc.csic.es

Portland cement pastes when exposed to acid solutions.

Another important issue in connection with the durability of these new materials is their sensitivity to the alkali–silica reaction (due to their high alkali content: ≥8% Me_2O); given the small amounts of CaO in this type of materials, however, they may be expected to behave differently than OPC concretes in this regard. And indeed, Lodeiro et al. [16] when applying standard C1260-94 found that 8 M NaOH-activated fly ash mortars expanded less than OPC.

In light of the knowledge gaps around the durability of these materials, the present study focused on the resistance of alkali-activated type F fly ash mortars to chemical attack by aggressive leaching agents (seawater, sulphates, acids) and expansion due to possible alkali–silica reactions.

Experimental

Materials

A Spanish fly ash (type F according to ASTM C618-03) was used in this study. Table 1 gives the chemical composition, while a full characterization can be found in [17]. One important property of this fly ash in the present context is that approximately 90% of the particles are smaller than 45 μm and 50% are less than 10 μm. The control mortars were made with type I Portland cement, chosen for its low alkali content (see Table 1).

Two alkali activating solutions were used: N = 8 M NaOH and W = mixture 85% 12.5 M NaOH + 15% sodium silicate (SiO_2/Na_2O = 0.16). The components used to prepare the alkaline solutions were (98% pure) NaOH and sodium silicate (8.2% Na_2O, 27% SiO_2 and 64.8% H_2O, d = 1.38 g/cc).

Methods

Resistance to chemical attack: static test

Prisms measuring 4 cm × 4 cm×16 cm with solution/ash ratios of 0.35 (for solution N) and 0.4 (for solution W) were prepared to determine the performance of these materials when exposed to sulphates and sea- and deionized water. The mortars, which contained sand with a 95% quartz content (see standard CEN EN 196-1), had a sand/ash ratio of 2/1. These (4×4×16-cm^3) mortar specimens were cured in an oven for 20 h at 85 °C and a relative humidity of 99%. They were subsequently demoulded and immersed in the respective aggressive media. Seven, 28, 56, 90, 180, 270 and 365 days after immersion, the specimens were removed from the aggressive environment, mechanically tested (bending and compressive strength as described in Spanish standard UNE-80-101-88) and characterized for their mineralogical composition.

The aggressive environments tested were: *A* = laboratory conditions (control); *H* = deionized water; *M* = seawater (ASTM D 1141-90); and *S* = sodium sulphate solution (4.4% Na_2SO_4)

Acid attack (0.1 N, pH 1.0 HCl solution): dynamic test

To determine performance of the material under acid attack (0.1 N, HCl solution pH 1.0), a dynamic test based on the ANS 16.1 [18] method for measuring leachability was conducted on 3×3-cm^2 cubic mortar specimens prepared as discussed in the preceding item. A Portland cement mortar with a sand/cement ratio of 3/1 and a water/cement ratio of 0.35 was used as a control.

The acid solution volume/specimen surface area ratio was set at 10. The acid was poured off and replaced with fresh solutions after 1, 2, 3, 7, 28, 56, and 90 days. Specimens were tested after 7, 28, 56 and 90 days for variations in weight and mechanical strength. Mineralogical and microstructural characterizations were also performed.

Alkali–silica reaction

Material stability in the presence of the alkali–silica reaction was determined with an accelerated test based on the procedure described in ASTM standard C1260-94. The mortar specimens (2.5 × 2.5 × 28.5-cm^3 prisms) made for this purpose had an aggregate/ash

Table 1 Chemical composition of materials used

	L.o.I	IR	SiO_2	Al_2O_3	Fe_2O_3	CaO	MgO	SO_3	K_2O	Na_2O	Others
Fly ash[a]	3.59	0.32	53.09	24.80	8.01	2.44	1.94	0.23	3.78	0.73	1.07
Cement	–	1.44	21.5	3.31	2.67	66.2	1.01	2.93	0.57	0.085	0.28
Siliceous Aggregate	17.4		48.5	6.94	2.58	21.1	0.93	0.06	1.38	0.67	0.06

L.o.I. loss on ignition, *IR* insoluble residue

[a] Reactive SiO_2 calculated as specified in Spanish standard UNE 80-225-93 = 50.44%

ratio of 2.25/1 and solution/ash ratios of 0.47 for solution N and 0.64 for solution W. The aggregate was a siliceous mineral commonly used to make concrete in Spain and generally regarded to be non-reactive [16]. This aggregate was crushed, ground and sieved to the particle size distribution specified in the standard. Its chemical composition is given in Table 1. The mortars were initially cured for 20 h at 85 °C and a relative humidity of 99%. After demoulding, the specimens were submerged in a 1 M NaOH solution and stored in sealed containers in an oven at 85 °C. This method estimates the deterioration that ASR may potentially cause in cement mortars in 16 days. Variations in specimen length were determined periodically to calculate possible expansion. EDX and SEM/EDX studies were likewise run.

In this case a Portland cement mortar with a sand/cement ratio of 2.25/1 and a water/cement ratio of 0.47 was used as a control.

Characterization techniques

The mineralogical and microstructural characteristics of the materials were studied by means of XRD and SEM/EDX. X-Ray diffraction patterns of powdered samples were obtained with a Philips PW 1730 diffractometer, using CuKα radiation. Specimens were step-scanned at 2° min^{-1}, with 2θ in the 2–60° range, a divergence slit of 1°, anti-scatter slit of 1° and receiving slit of 0.1 mm. Finally, a JEOL JSM 5400 scanning electron microscope equipped with a LINK-ISIS energy dispersive (EDX) analyser was used for microstructural characterization.

Results

Resistance to chemical attack (sulphates and seawater)

Figure 1 shows the compressive strength developed by the AAFA mortars made with the two alkaline solutions (N and W) after each period of immersion in the various aggressive solutions. As a general rule, the mortars made with solution W exhibited higher strength values than the ash activated with solution N. The results also show that the materials did not deteriorate significantly, although mechanical strength was observed to fluctuate in the early ages (see Fig. 1). The strength increases over time were of the same order of magnitude irrespective of the medium in which the specimens were immersed.

Figure 2 gives the XRD spectra for the original ash and the samples studied. The original fly ash essentially comprised a majority vitreous phase (see the hump at 2° = 20°–30°) and a number of minority crystalline phases: quartz, mullite, hematite, and some CaO (see spectrum FA in Fig. 2). When the fly ash was activated under the above conditions, regardless of the activating solution used (N or W), the reaction product formed was an alkaline aluminosilicate gel with a low-order crystalline structure. In the X-ray diffractograms, the characteristic hump for amorphous or vitreous phases partially overlapped with the hump from the original ash, which the activation reactions shifted towards slightly higher 2θ values (from 20°–30° to 25°–35°, see spectrum A in Fig. 2). New minority crystalline phases, namely hydroxysodalite ($Na_4Al_3Si_30_{12}OH$) and herschelite ($NaAlSi_2O_6 \cdot 3H_2O$) were also identified. The intensity of the peaks corresponding to these zeolites increased with curing time [19–21].

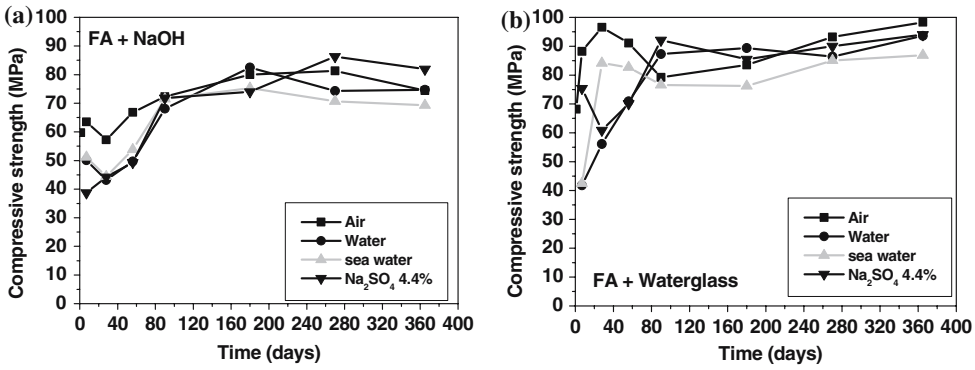

Fig. 1 Mechanical strength of (**a**) ash mortars activated with an 8 M NaOH solution, (**b**) mortars activated with a 15% solution of sodium silicate + 85% 12.5 M NaOH

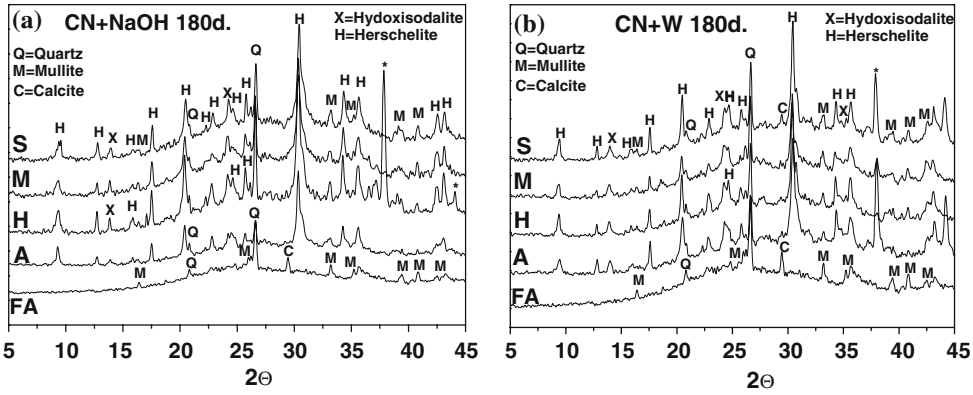

Fig. 2 XRD spectra after 180 days for (**a**) ash activated with solution N; (**b**) ash activated with solution W; *FA* original fly ash; *A* cured under laboratory conditions; *H* immersed in deionized water; *M* immersed in seawater; *S* immersed in a sodium sulphate solution

Figure 2 also shows the spectra obtained for the different matrices 3 months after immersion in deionized water, seawater and a sodium sulphate solution (patterns H, M and S, respectively). No significant mineralogical changes were observed in the materials as a result of immersion; the main reaction product in all cases was an aluminosilicate gel, with herschelite and hydroxysodalite as secondary crystalline phases.

No signs of surface deterioration were found in a visual inspection of the mortar prisms after immersion in the various aggressive media for one year. A more detailed microstructural study did reveal certain alterations, however. Figure 3 shows the morphology of the ash activated with solution W after one year of immersion in sulphate sodium solution and Fig. 4 shows the same ash after 12 months in seawater. In both images, the appearance of the cementitious material is typical of ash activated with waterglass [4, 22]: the majority product, a sodium silicoaluminate gel, is found alongside herschelite-type zeolites, also a minor content of P zeolite was observed by SEM. The only variation on this type of microstructure is the presence of unreacted ash particles, and/or microfissures. Such fissures are regarded to be the result of a series of internal stresses arising in the material during microstructural development and not generated by the medium in which the specimens were immersed, inasmuch as they were also found in the control matrices (*A* = laboratory conditions) and in previous studies [4, 22].

Finally, 1 year after immersion, SEM analysis detected sodium sulphate crystals in the specimens kept in the sodium sulphate solution. These crystals appeared inside unreacted ash or in the spaces they left after the particles had reacted (see Fig. 3b). A silicon-rich gel with some magnesium was also observed to

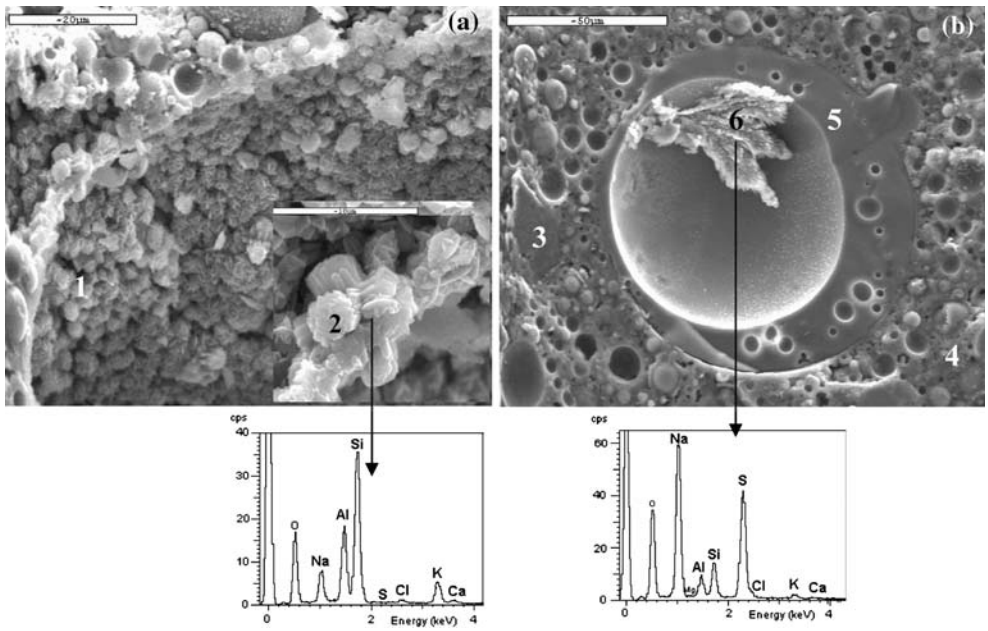

Fig. 3 SEM images of FA + W mortar immersed in sodium sulphate solution for 365 days: (**a**) P1 = herschelite-type zeolite; P2 = zeolite P; (**b**) P3 = aggregate; P4 = matrix; P5 = unreacted fly ash; p6 = sodium sulphate crystals

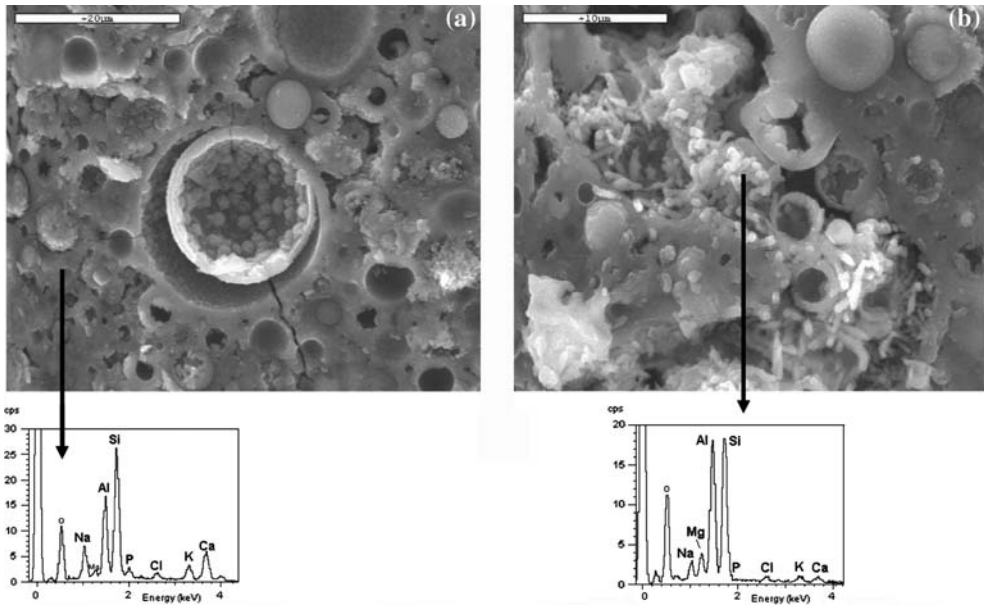

Fig. 4 SEM images of FA + W mortar immersed in seawater for 365 days

appear sporadically in the specimens immersed in seawater (Fig. 4b).

Acid attack (0.1 N, pH 1.0 HCl solution): dynamic test

At given intervals throughout this test, the HCl was replaced with a fresh solution (see experimental). A parallel study was likewise conducted with Portland cement mortars (control). The compressive strength results obtained are given in Fig. 5. According to these findings the strength values for all the mortars studied followed a downward pattern during the test. In the fly ash mortars activated with solutions N and W, however, strength declined by approximately 23–25%, whereas in the OPC mortars strength dropped at nearly twice that rate (47%). This decline in strength values went hand-in-hand with a decrease in specimen mass: the 90-day weight loss in mortars made with solution N-activated fly ash came to 2.5% compared to 4.2% for solution W-activated ash. The loss in OPC mortars was 9.8%.

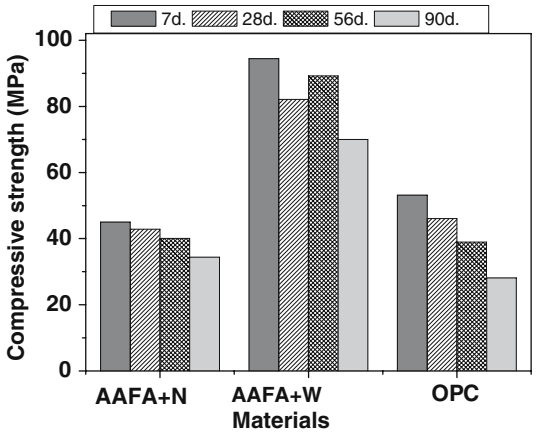

Fig. 5 Mechanical strength of AAFA and OPC mortars attacked wit h a 0.1 N solution of HCl

The XRD results in this case revealed important changes in the mineralogy of mortars activated with both solution N and solution W. More specifically, the peaks associated with the zeolitic phases tended to disappear with time (see Fig. 6). When W was the activator, a certain amount of zeolite (herschelite) was still detected 7 days after immersion, but as the test progressed, the intensity of the signals decreased and practically vanished altogether after 90 days. At the same time, the area of the amorphous halo was observed to grow.

A visual examination of the specimens exposed to acid solutions showed that while the AAFA specimens (whether activated by solution N or solution W) appeared to be healthy after 90 days, the OPC specimens were severely deteriorated after 56 days of immersion, with a conspicuous colour change and a loss of mass around the edges of the cubes (see Fig. 7).

Micrographs of exposed and unexposed samples of solution W-activated fly ash 90 days after preparation are given in Fig. 8. While the cementitious matrix was fairly compact in both samples, it was more porous in the specimen immersed in the acid. Electron microscopic studies detected herschelite-type zeolites in both matrices. The most notable difference was found, however, in the microanalysis of the matrix. In the samples immersed in the HCl solution, the aluminium

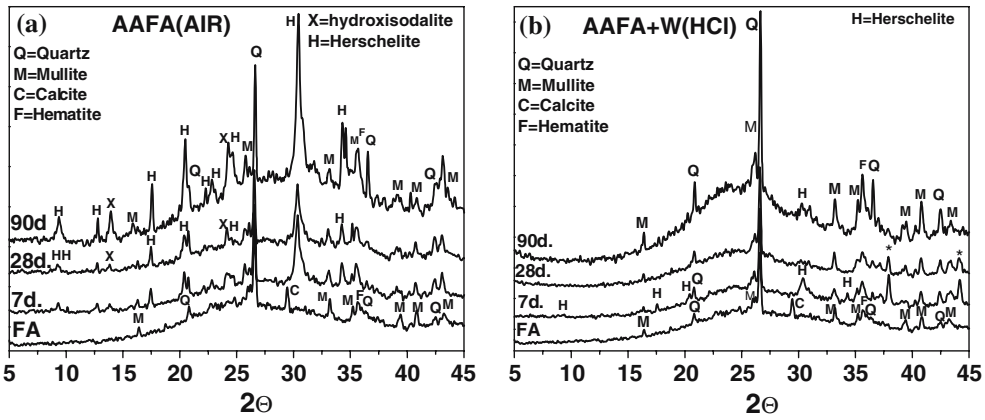

Fig. 6 XRD spectra for solution W-activated fly ash (**a**) cured in the laboratory and (**b**) immersed in 0.1 N HCl

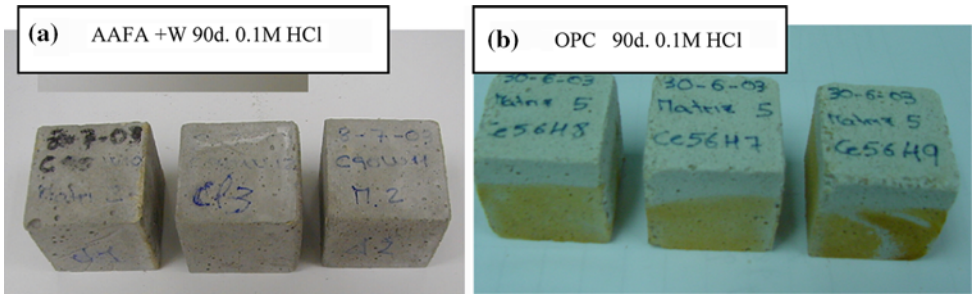

Fig. 7 Physical appearance of the mortar specimens after immersion for 90 days in a 0.1 N solution of HCl (**a**) solution W AAFA mortars and (**b**) OPC mortars (control)

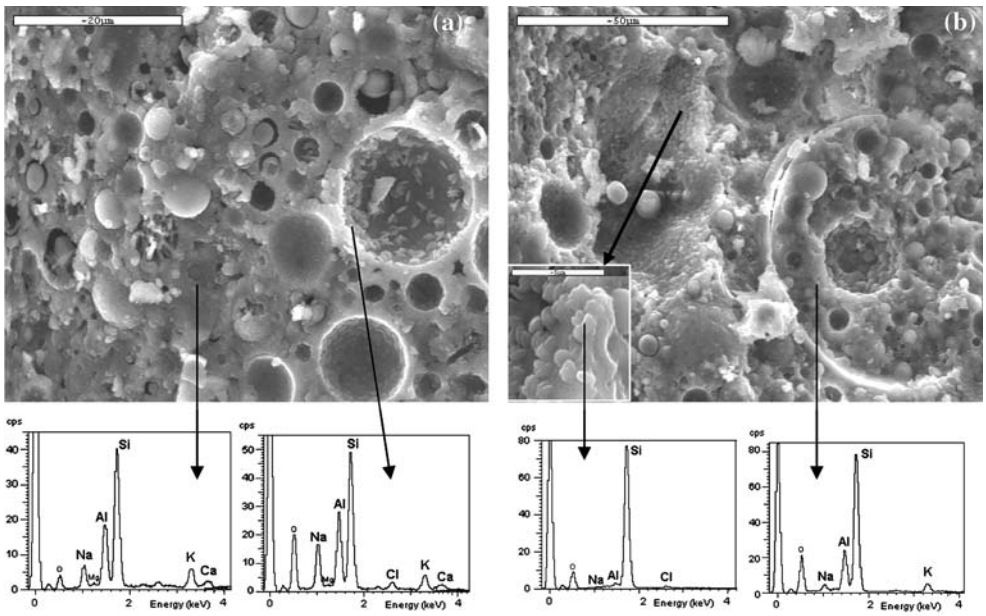

Fig. 8 Micrographs and EDX analysis of solution-W activated fly ash at the age of 90 days (**a**) not exposed to HCl and (**b**) immersed in HCl (dynamic test)

content in the gel and zeolites dropped substantially: in other words, the specimens were dealuminated (see Fig. 8). Similar results were obtained for solution N-activated specimens.

Alkali–silica reaction

An accelerated test based on the procedure described in ASTM standard C1260–94 was conducted to study

the possible ASR-mediated expansion of mortars. A potentially non-reactive aggregate was used in this part of the study, although prior analysis revealed the presence of some reactivity due to its cryptocrystalline quartz macle content and stressed. The accelerated test results showed that both mortars (activated with solutions N and W) performed well under conditions favouring the alkali–silica reaction, expanding less than the 0.1% limit stipulated in the standard after 16 days (see Fig. 9). The specimens tested appeared to be healthy, with no surface cracking.

In 1958 Plum y Poulsen [23] established the following general equation:

$$Ca(OH)_2 + SiO_2 + Na(OH) + H_2O \rightarrow n_1Na_2O \cdot n_2CaO \cdot n_3SiO_2 \cdot n_4H_2O \text{ (gel-type product)}$$

where the gels formed are more or less expansive depending on the CaO content. However, while the presence of calcium appears to be essential for the ASR gel to expand, the role of this element in the reaction mechanism continues to be a matter of controversy [24, 25]. According to Davis y Oberholster [26], the ASR gel can be different type of morphology. rosette, rod-like type gel. In the materials subjected to accelerated testing for 16 days no typical ASR products were detected by SEM/EDX.

Zeolitic crystalline phases such as hydroxysodalite, herschelite and zeolite P were detected along with the hydrated sodium aluminosilicate gel, however (see Fig. 10a). Zeolite P, with a Si/Al ratio of 2.49 and a Na/Al ratio of 1.15, had not been observed previously (data confirmed by XRD, see Fig. 11). The presence of zeolite P can be explained by the very aggressive conditions to which the specimens were subjected [27–30].

At older ages (180 days) some expansion was observed. SEM/EDX and XRD characterization of these specimens led to essentially two findings: (1) the formation of a small amount of alkali–silica reaction product (see Fig. 10b), with a Ca/Si ratio of 0.15, a Na/Si ratio of 0.72 and crystals with a pseudo-rosette morphology [16]. On occasion, the gels so formed were fluid enough to seep through the cracks and partially or wholly occupy gaps in the matrix, thereby attenuating expansion. (2) After 180 days of storage in 1 M NaOH at 85 °C, a new zeolitic phase was detected, analcime, with a Si/Al ratio of 2.40 and a Na/Al ratio of 1.26 (see Fig. 10c).

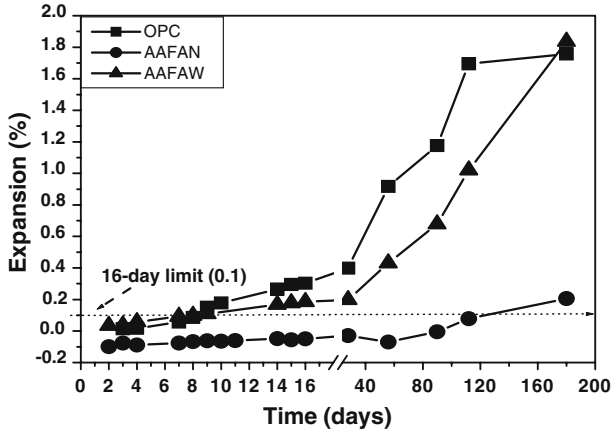

Fig. 9 Alkali–silica reaction-induced expansion determined by the accelerated test based on ASTM standard C1260-94

Discussion

Since the durability of any material is closely related to its mineralogical composition and microstructure, the significant differences found in this regard between Portland and AAFA cements cannot be regarded to be unexpected, given the substantial differences between the reaction products formed in each case.

Many of the durability problems posed by OPC are associated in one way or another with the calcium content of its main phases. Sulphate attack by ions in the soil as well as in ground- and seawater deteriorates reinforced concrete structures, for instance. In hardened cement, C_3A reacts with sulphate ions in the presence of $Ca(OH)_2$ to form ettringite and gypsum, leading to the disruptive expansion of concrete and its degradation into a non-cohesive granular mass [31–35]. Another important example is reinforcement corrosion, a process triggered in most cases by the carbonation of $Ca(OH)_2$, which in turn leads to a decline in the pH of the cementitious matrix [36]. Finally, most authors believe that Ca, along with other factors such as damp, the presence of alkalis, potentially reactive aggregate and so on, is also necessary for the alkali–silica reaction to take place [31, 32].

Consequently, the low Ca content in AAFA cements is a very important characteristic in this regard. Indeed, in this case the main reaction product is an alkaline aluminosilicate gel with a three-dimensional structure (considered to be a zeolite precursor) [19, 20], which is distinctly different from the C–S–H gel formed in OPC hydration.

Sulphate and seawater attack

Generally speaking, the mortars activated with both solution N and solution W performed well in the various media studied, with mechanical strength values increasing with time. Strength was observed to dip

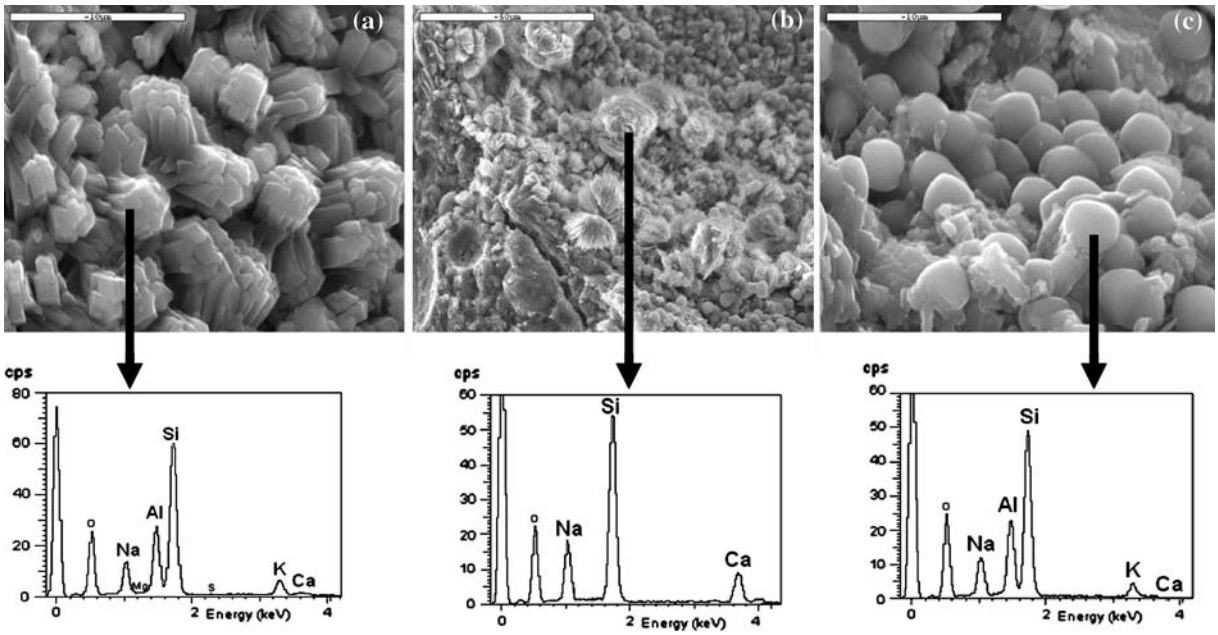

Fig. 10 SEM micrographs and microanalysis of solution N-activated fly ash mortar subjected to the accelerated test (ASTM C1260-94): (**a**) zeolite P crystals observed after 16 days; (**b**) alkali–silica reaction product with pseudo-rosette crystals after 180 days; (**c**) analcine crystals after 180 days

slightly only after 7 days in specimens in which N was the activator and after 28 where W was the activator. These fluctuations should not be attributed, however, to the medium in which the samples were immersed, since they were also detected in the control specimens (cured under laboratory conditions). The reasons for such variations, also observed for metacaolin-based geopolymers [11], are not clear and will be addressed in greater detail in the near future. In any event, the mortars activated with solution W (which includes soluble silicates) appeared to exhibit the highest strength values in all the media studied.

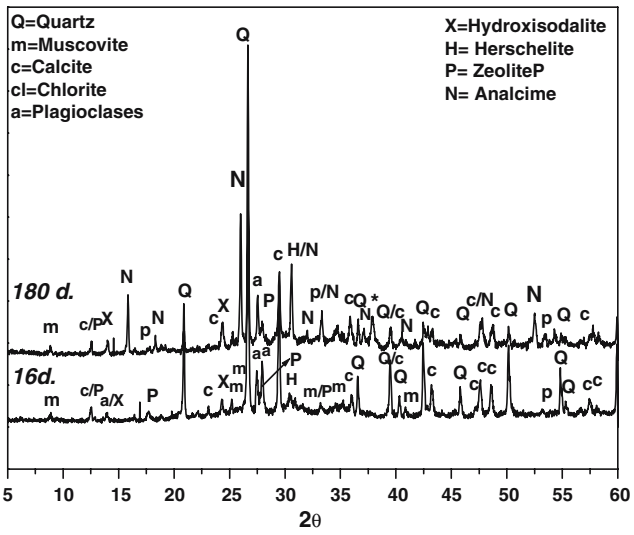

Fig. 11 XRD spectrum of solution N-activated fly ash mortars immersed in a 1 N NaOH solution at 85 °C for 16 and 180 days

No significant differences were observed in gel composition or microstructure after contact with saline solutions. Nonetheless, the presence of phases such as sodium sulphate was detected in some cases, associated less with the degradation of the matrix than with the inward migration of sulphate ions through its porous structure. Due to the large amount of Na in the system, these sulphate ions precipitate into the gaps or pores in the matrix in the form of sodium sulphate.

In the specimens immersed in seawater, magnesium ions in the solution also were also observed to seep into the matrix. In this case, since the process appears to involve an exchange of Mg and Na ions, it introduces changes in gel composition and morphology. These reactions are very sporadic, however, and seem to have no significant effect on mechanical strength.

The performance differences in durability tests depending on the activator used (N or W) are due in part to the structural variations in the alkaline silicoaluminate gel formed as a result of the different Si/Al ratios induced in the system, as well as to the larger or smaller amounts of (zeolite) crystalline phases in the matrix. It is a known fact that the presence of soluble silicates in the activating solution generally reduces the degree of alkaline silicoaluminate crystallization and

retards zeolite crystallization [37, 38]. Prior research has shown, however, that when the silicate ions present in the alkaline activating solution reach a threshold value, gel and zeolite crystallization processes in particular are favoured [4, 8, 38, 39] (see Fig. 2). Moreover, the presence of silicate ions leads to the formation of more compact structures (see Figs. 3, 4), with gels richer in Si [7, 22]. This would explain why mechanical strength is higher in mortars activated with solution W than with solution N.

Stability in an acid medium

Of all the aggressive media tested in this study, the 0.1 N HCl solution is the one with the greatest capacity to dissolve materials. Another fact to be borne in mind in this regard is that in the acid attack test the leaching agent was renewed periodically.

Treatment with HCl is a well-known and commonly used dealumination procedure to obtain silica-rich zeolites [37, 38]. In the present research, the process that may have been prompted by the interaction between the reaction products and the acid solution used was the replacement of exchangeable cations (Na, K) with hydrogen or hydronium ions [38].

Treating the inorganic polymer with a highly acidic solution triggers a direct attack on and concomitant dealumination of the silicoaluminate structure. Such an attack appears to break the Si–O–Al bonds, increasing the number of Si–OH and Al–OH bonds, which in turns raises the number of silicic acid ions and dimers in the solution. This process ultimately leads to a loss of mass in the polymeric structure (2.5% in mortars activated with solution N and 4.2% in those activated with solution W).

Due to the low pH values of the aggressive medium, aluminosilicate depolymerization was followed by condensation of silicon-enriched polymeric ions (see Fig. 8). The AAFA mortars nonetheless performed better than the OPC mortars, which proved to be less durable in acid media in which, all other conditions being equal, OPC mortars lost 9.8% of their mass and 47% of their strength. Further to the literature on the subject [36], the mechanisms governing acid attack in OPC mortars are entirely different from the process in AAFA mortars.

Volume instability due to the alkali–silica reaction

Deterioration in OPC-based concrete consisting in expansion, cracking, loss of mechanical strength, elasticity and durability is an outcome of the reaction between the alkaline ions from the Portland cement or other sources and the siliceous components of certain types of aggregate. This process, known as the ''alkali–silica reaction'', depends on factors such as the presence of potentially reactive aggregate, the existence of alkalis in the medium ($Na_2O + K_2O$), damp and so on. The absence of any of these factors reduces or may even prevent the reactive process and consequently expansion. Some authors [31, 32] sustain that the alkalis present in the porous solution and the reactive silica of the aggregate are not the only factors involved in ASR, but that Ca-rich phases such as the portlandite ($Ca(OH)_2$) generated during Portland cement hydration are requisite to the reaction.

Ash matrices have a high alkali content but a very low Ca content. For this reason, with potentially non-reactive aggregate such as normally used to manufacture OPC concrete, expansive sodium–calcium silicate gels are unlikely to form. According to the graph in Fig. 9, the expansion recorded in AAFA mortar after 16 days plainly did not exceed the limit established in the accelerated method.

Figure 9 also shows, however, that after 180 days of accelerated testing, expansion in the prisms exceeded that ceiling (regardless of the type of activating solution used). Such expansion was nonetheless less intense than in OPC mortars under similar conditions. According to the authors of this study, a number of reasons may explain this expansion when the duration of the accelerated test is extended. Firstly, the ASTM C1260 test is ''extremely'' aggressive, with specimens immersed in a 1 M solution of NaOH at a temperature of 85 °C. Such severe conditions are known to substantially accelerate the formation of ASR expansive products in OPC systems [31, 32]. The same may occur in the AAFA systems, where ASR product was detected, albeit in small amounts.

SEM observations, in turn, showed that in addition to the sodium silicoaluminate, zeolitic crystalline phases were formed. The quantity and type of such phases varied with test time. As they were usually found to precipitate into gaps in the matrix, no stress was generated in the material that might lead to microfissures; rather, these phases had a beneficial effect on mechanical strength by plugging pores.

Herschelite and hydroxysodalite were the zeolites normally appearing in these systems [4, 19, 20]. Sixteen days after subjecting the materials to the accelerated test (ASTM C1260), however, zeolite P was detected among the crystalline phases formed, whereas analcime prevailed after 180 days (see Fig. 11). Moreover, the substantial amounts of these larger

zeolites appearing were not always located in gaps. This zeolite transformation is believed to be the cause of a certain amount of stress, which would contribute to the expansion detected. There is evidence, then, that on the one hand the low Ca content in these systems greatly minimizes possible expansion by alkali–silica reactions that might otherwise be expected to take place in light of the high concentration of alkalis in the system; and on the other the intrinsic characteristics of the ASTM C1260-94 accelerated test may cause an overlapping of two effects: formation of expansive products by ASR and/or of zeolites.

Conclusions

The chief conclusions to be drawn from the present study are as follows:

- Alkali-activated fly ash mortars, regardless of the type of activator used, are generally more durable than OPC mortars under the experimental conditions analyzed in this study.
- Since the mineralogical phases and characteristic microstructural elements of AAFA pastes and mortars are very different from the properties of OPC mortars, the degradation processes differ in the two types of material.
- AAFA pastes and mortars perform satisfactorily when exposed to sulphates and seawater. In the presence of sulphates, small amounts of sodium sulphate are formed as a degradation product. In seawater Na ions are replaced by Mg ions, making the gel microstructure slightly more porous.
- AAFA pastes and mortars undergo dealumination in highly acidic media. This entails a loss of mass and a decline in mechanical strength. Performance is still better, however, than observed in OPC mortars.
- In connection with alkali–silica reaction-induced expansion, these mortars are within the 16-day limit specified in ASTM standard C1260-94. The expansion observed when the duration of the accelerated test is extended may be explained by the overlapping of two effects: ASR and/or zeolite growth.

Acknowledgements This study was funded by the General Direction of Scientific Research (project BIA2004-04835). The CSIC and the European Social Fund co-financed an I3P contract (REF. 13P-PC2004L) in connection with this research. The authors wish to thank J. García and A. Gil for their assistance in the preparation of the mortar specimens.

References

1. Krivenko PV (1992) Proceedings of the 4th CANMET-ACI international conference on fly ash, silica fume, slag and natural pozzolans in concrete, Istanbul, p 721
2. Palomo A, Grutzeck MW, Blanco MT (1999) Cem Concr Res 29:1323
3. Xu H, van Deventer JSJ (2000) Int J Miner Process 59:247
4. Fernández-Jiménez A, Palomo A (2005) Cem Concr Res 35:1984
5. van Jaarsveld JGS, van Deventer JSJ (1999) Ind Eng Chem Res 38:3932
6. Lee WKW, van Deventer JSJ (2002) Colloids Surf A: Physicochem Eng Aspects 211:49
7. Criado M, Palomo A, Fernández-Jiménez A (2005) Fuel 84:2048
8. Fernández-Jiménez A, Palomo A, Sobrados I, Sanz J (2006) Microporous Mesoporous Mater 91:111
9. Fernández-Jiménez A, Palomo A, Criado M (2005) Cem Concr Res 35:1204
10. Zhaohui X, Yunping X (2001) Cem Concr Res 31:1245
11. Palomo A, Blanco-Valera MT Granizo ML, Puertas F, Vázquez T, Grutzeck MW (1999) Cem Concr Res 29:997
12. Bakharev T (2005) Cem Concr Res 35:658
13. Bakharev T (2005) Cem Concr Res 35:1233
14. van Jaarsveld JGS, van Deventer JSJ, Lorenzen L (1998) Metall Mater Trans B: Process Metall Mater Process Sci 29(1):283
15. van Jaarsveld JGS, van Deventer JSJ (1999) Ind Eng Chem Res 38(10):3932
16. García-Lodeiro I, Palomo A, Fernandez-Jimenez A (2005) RILEM congress ''concrete and reinforced concrete''. ISBN 5–98580-013-X, vol 4, p 452
17. Fernández-Jiménez A, Palomo A (2003) Fuel 82:2259
18. Conner JR (1990) Ed. Van Nostrand Reinhold, New York
19. Palomo A, Alonso S, Fernández-Jiménez A, Sobrados I, Sanz J (2004) J Am Ceramic Soc 87(6):1141
20. Fernández-Jiménez A, Palomo A (2005) Microporous Mesoporous Mater 86:207
21. Murayama N, Yamamoto H, Shibata J (2002) Int J Miner Process 64:1
22. Palomo A, Fernández-Jiménez A, Criado M (2004) Mater Construc 54:77
23. Plum DW, Poulsen E (1958) Ingeniorum Int Ed Danemark 2:26
24. Dent Glasser LS, Kataoka (1982) Cem Concr Res 12:321
25. Chatlerji S (1979) Cem Concr Res 9:185
26. Davies G, Oberholster RE (1988) Cem Concr Res 18:621
27. Vucinic D, Miljanovic I, Rosic A, Lazic P (2003) J Serb Chem Soc 68(6):471
28. Tanaka H, Matsumura S, Hino R (2004) J Mater Sci 39(5):1677
29. Molina A, Poole C (2004) Miner Eng 17:167
30. Tanaka H, Miyagawa A, Eguchi H, Hino R (2004) Ind Eng Chem Res 43(19):6090
31. Swamy RN (1992) Cap.1 Swamy, R.N. Ed. Blackie, New York, p 96
32. Johansen V, Thaulow N, Skalny J (1993) Adv Cem Res 5:23–29; (b) unpublished data from evaluation of industrial concrete products
33. Lawrence CD (1995) In: Skalny J, Mindess S (eds) Materials science of concrete IV. The American Ceramic Society, Westerville, OH, p 113

34. Marusin SL (1995) In: Gouda G, Nisperos A, Bayles J (eds) Proceedings of the 15th international conference on cement microscopy, ICMA, 1993, p 289; see also ''Deterioration of railroad ties in the USA'', 1995. In: Proceedings of the CANMET/ACI international workshop on AAR in concrete. Nova Scotia. p 243
35. Taylor HFW (1994) In: Grutzek MW, Sarkar SL (eds) Advances in cement and concrete. American Society of Civil Engineers; see also ''Sulphate reactions—microstructural and chemical aspects''. Cement Technol Ceram Trans 40:61
36. Neville AM (1995) Ed. Logman, Essex
37. Engelhardth G, Michel D (1987) Ed. Wiley, New York
38. Klinowski J (1984) J Prog NMR Spectrosc 237
39. Duxson P, Provis JL, Lukey GC, Mallicoat SW, Kriven WM, van Deventer JSJ (2005) Colloids Surf A: Physicochem Eng Aspects 269(1–3):47